한국부식학회지
J. Corros Sci. Soc. of Korea
Vol. 24 No. 1, March, 1995
〈總 說〉

금속의 양극산화중 금속표면에 발생되는 응력에 대한 개요

金 重 道·邊 秀 一
韓國科學技術院 材料工學科

A Review of Stress Generation during Anodic Oxidation of Metals

JOONG-DO KIM and SU-IL PYUN
Department of Materials Science and Engineering,
Korea Advanced Institute of Science and Technology,
#373-1 Kusong Dong, Daejon 305-701, Korea

1. Introduction

The application of anodic current or anodic potential to a number of metals results under suitable conditions in the formation of continuous and protective surface oxide layer, known as barrier oxide or passive films. These oxide films are of commercial importance as well as scientific interest because of their dielectric and semiconducting behaviour applicable to electronic components such as capacitors, MOS device and small area display etc.[1,2]

When metals are anodized to form barrier oxide films, growth of these films is generally accompanied by a development of internal stresses in the oxides. The stresses are often quite large and may exceed the strength of the film, resulting in cracking, an interface may fail, resulting in delamination.[3] The problems become evident during process developments and make an otherwise attractive process nonviable. So, extensive works[3-8] have been carried out to elucidate the mechanisms of stress generation, of stress relief, and of oxide film failure. Even though a great number of propositions[3-8] have been suggested about the nature of surface stresses, there are as yet many ambiguities and controversy concerning the magnitude and sign of surface stresses in anodic oxide films.

So, in order for a complete understanding of surface stresses in anodic oxide films on metals, it will be discussed firstly about well established sources of stresses in growing oxide films and then discussed in detail experimental grounds for measuring the stresses. Finally, because the stress changes are closely related to the film formation variables of applied current density and electrolyte composition, it will briefly be described in terms of growth kinetics of anodic oxide films on metals.

2. Discussion

2.1 The Pillings-Bedworth model

Pillings and Bedworth[9] theorized that protective films on metals formed because the oxide produced was of a greater volume than the metal which it replaced, generating a compressed compact layer at the surface which impeded further transport of the reacting species. The Pillings-Bedworth Ratio(PBR), is defined as follows:

$$PBR = \frac{molar\ volume\ of\ metal\ oxide}{molar\ volume\ of\ metal} \quad (1)$$

Table 1[10] shows the typical values of PBR. It can be seen that this model predicts that the growth stresses in MgO will be tensile, and those in FeO and Ta_2O_5 compressive. However, the magnitude of the volume change is so great that it seems impossible that the model can be correct as it stands : quite thick layers of anodic oxide films can be grown without fracture, suggesting that the actual stresses are much less than those suggested by the Pillings-Bedworth model.

Table 1. The Pillings-Bedworth Ratio(PBR) of various metal-metal oxide systems taken from Kubaschewski and Hopkins[10]

Metal-Metal Oxide	PBR
Li-Li_2O	0.58
Mg-MgO	0.81
Al-Al_2O_3	1.28
Zn-ZnO	1.55
Ni-NiO	1.65
Fe-FeO	1.70
Ti-TiO_2	1.73
Ta-Ta_2O_5	2.50
W-WO_3	3.34

2.2 Stress due to Coulomb force

One source of surface stress in growing oxide film is directly due to the electric fields present in the oxide film layer.[11] The relationship between surface charge density and electric field is given by Gauss Law,[12]

$$E = \frac{4\pi}{\varepsilon} qN \quad (2)$$

where E is the electric field, N is the number of particles of charge q per unit area and ε is the dielectric constant of the oxide film layer. The force exerted on a single charge q at one interface is 0.5qE, so the force exerted on the number of charged particles N covering unit area of one interface is 0.5 qEN. Hence the electrostrictive stress σ_{coul} exerted perpendicular to the plane of the oxide film layer produced by this effect is given by

$$\sigma_{coul} = \frac{\varepsilon}{8\pi} E^2 = \frac{\varepsilon}{8\pi} \frac{V^2}{d^2} \quad (3)$$

where V is the electrostatic potential(=E x d) and d represents the thickness of the oxide layer; any space charge within the oxide film layer is neglected for simplicity in this equation. This quantity has the dimensions of force per unit area, and it is independent of position within the oxide. As the oxide film layer is compressed it tends to expand in the plane of the oxide film but is constrained by the metal substrate, developing a lateral stress under plain strain condition which is given by[13]

$$\sigma_{coul} = \frac{\nu_{MO}}{1-\nu_{MO}} \frac{\varepsilon}{8\pi} \frac{V^2}{d^2} \quad (4)$$

where ν_{MO} is Poisson's ratio for the oxide film layer. Taking $E=10^6$ V/cm,[14] $\varepsilon=10^{15}$[15] and $\nu_{MO}=$

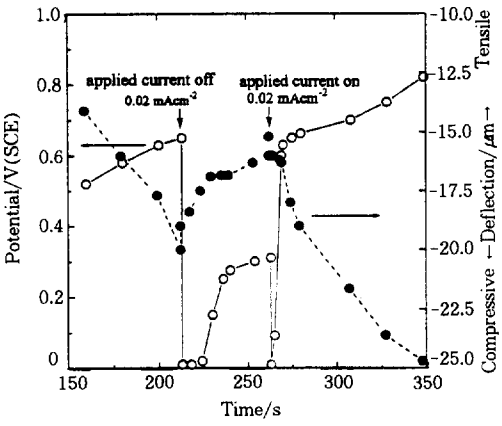

Fig. 1. Responses of potential(○) and deflection (●) to current interruption during anodic oxidation of tungsten strip specimen at an applied current density of 0.02mA cm^{-2}.

0.33,[16] a σ_{coul} of 1.73MPa is calculated. This value is relatively small as compared to the measured stress of a few GPa in anodic oxide films and is always compressive.

The effect of electrostriction during anodic oxidation of metals was noted in the previous works.[17,18] Figure. 1[18] shows open-circuit transients in voltage and deflection recorded during anodic oxidation of tungsten at a current density of 0.02 mA ·cm^{-2} After interrupting the applied current density, the relaxation of electrostriction as the potential dropped produced an instantaneous tensile movement followed by a further tensile movement which declined to the steady state. The instantaneous tensile movement indicates that an electrostrictive force acts as a compressive stress component during the oxide film growth. The further tensile movement was attributed to the relaxation of elastic stress of the tungsten/anodic tungsten oxide film system.[19]

2.3 Determination of stresses in oxide films based upon curvature measurement

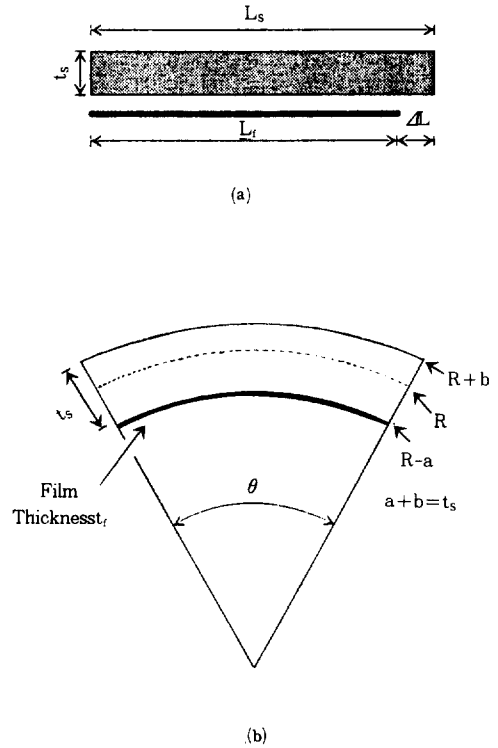

Fig. 2. A schematic representation of a bending of a strip taken from Flinn et al.[20] (a) Unconstrained substrate(shown crosshatched) of length L_s, and unconstrained film(shown below and detached from substrate) of lenqgth L_f; the length difference is ΔL. (b) Film constrained to match substrate and composite structure allowed to relax to configuration of minimum energy. R is the radius at which the substrate arc is the same length as in the unreformed material; a is the distance from the inner surface of the substrate to R and b is the distance from R to the outer surface. The film thickness t_f is much less than the substrate thickness, t_s. The angle of bending, θ, and the value of a are such as to minimize the total energy of the system.

Figure 2[20] shows a simple one-dimensional representation of a thin film of thickness t_f on a substrate of thickness t_s. The unconstrained length of the film would be L_f and that it must be stretched by an amount ΔL to match the length L_s of the

substrate as shown in Fig.2(a). The deformed film attached to an undeformed substrate does not represent a condition of minimum energy; the energy of the entire system can be lowered by deforming the substrate slightly so as to reduce the deformation of the film. This deformation has two components: an overall compression of the substrate and bending of the substrate. The combined effect is shown in Fig. 2(b).

The distance from the center of curvature to any point in the material is r. R is defined as the radius at which the corresponding arc is of the same length as it was in the undeformed substrate. The portion of the substrate with radius r $<$R is under compression and with r$>$R is under tension. The situation with R at the center of the substrate thickness would correspond to pure bending. For the case we are considering, net compression, the distance a, which is from R to the inside of the substrate, is larger than half of the substrate thickness, while b, the distance from R to the outside of the substrate, is correspondingly smaller.

The change in length relative to the undeformed material along any arc of the substrate is given by

$$\Delta L=(r-R)\theta \tag{5}$$

where the θ is the angle of bending, and the corresponding elastic energy U in an arc of thickness dr is

$$dU=\frac{E_s}{2}(r\theta-L_s)^2dr \tag{6}$$

where E_s is the elastic modulus of the substrate.

The total elastic energy in the substrate is obtained by integrating Eq.(6) through the thickness, from (R-a) to (R+b), and is given by

$$U_s=\frac{E_s\theta^2}{6}(b^3+a^3) \tag{7}$$

Since the film is extremely thin relative to the substrate, the strain in the film is approximately uniform. The accommodation due to the bending is given by Eq.(5), with r-R=a, so that the net change in length of the film is given by

$$L_s-L_f-a\theta=\Delta L-a\theta \tag{8}$$

and the corresponding elastic energy of the film U_f is

$$U_f=\frac{E_f}{2}(\Delta L-a\theta)^2t_f \tag{9}$$

where E_f is the elastic modulus of the film and t_f is the film thickness. The total elastic energy of the system is now given by

$$U=\frac{E_s\theta^2}{6}(b^3+a^3)+\frac{E_f}{2}(\Delta L-a\theta)^2 \tag{10}$$

It is convenient to introduce the new variables

$$\left.\begin{aligned} x&=a-\frac{t_s}{2}\\ V&=x\theta\end{aligned}\right] \tag{11}$$

We can now express the total energy of the system in terms of θ, which measures the bending of the substrate, and V, which measures the overall compression of the substrate as follows:

$$\begin{aligned}U=&\frac{E_ft_f(\Delta L)^2}{2}+\frac{E_st_s^3\theta^2}{24}-\frac{E_ft_f\Delta Lt_s\theta}{2}\\&-E_ft_f\Delta LV+\frac{E_st_sV^2}{2}+\frac{E_ft_fV^2}{2}\\&+\frac{E_ft_ft_s^2\theta^2}{8}+\frac{E_ft_ft_sV\theta}{2}\end{aligned} \tag{12}$$

The last three terms have negligibly small values. We now find the value of the variableq that minimizes the total energy :

$$\frac{\partial U}{\partial\theta}=\frac{E_st_s^3\theta}{12}=\frac{E_ft_f\Delta Lt_s}{2}=0 \tag{13}$$

so that

$$\theta=\frac{6E_ft_f\Delta L}{E_st_s^2} \tag{14}$$

The stress σ_f in a film simply is given by the elastic modulus times the strain, so that

$$\sigma_f = \frac{E_f \Delta L}{L_s} \quad (15)$$

If we solve this equation for ΔL and substitute it in Eq.(14), we find

$$\theta = \frac{6 t_f \sigma_f L_s}{E_s t_s^2} \quad (16)$$

which gives us the well known result

$$\frac{1}{R} = \frac{\theta}{L_s} = \frac{6 t_f \sigma_f L_s}{E_s t_s^2} \quad (17)$$

or

$$\sigma_f = \frac{E_s t_s^2}{6 t_f R} \quad (18)$$

which is valid for a single uniform film.

If a film is in compression, rather than tension, the analysis is essentially the same; the substrate is bent in the opposite direction and is under net tension. Since 1/R is negative, the sign of stress is still given correctly by Eq.(18). If several films are present, we can treat the interaction of each film with the substrate separately. The stress in each film is determined by the misfit between that film and the substrate, and is independent of the other films. The total bending of the substrate is simply the linear combination of the contributions of the individual films determined separately. To determine the stress in a particular film, the inverse radius of curvature must be determined with and without that film. This change in 1/R is then used in Eq.(18) in place of 1/R to calculate the stress in that film.

The extension to two dimensions, at least for small deformations, is straightforward: Young's modulus (E) is replaced by the appropriate modulus for plane stress condition[21], $[E/(1-\nu_M^2)]$, where ν_M is the Poisson's ratio of metal substrate

$$\sigma_f = \frac{E_s t_s^2}{6(1-\nu_M^2) t_f R} \quad (19)$$

For single crystal substrates, E and ν_M are functions of orientation. Fortunately, if the crystal axis normal to the plane of the substrate has threefold or higher symmetry, as is commonly the case, the factor $E/(1-\nu_M^2)$ is isotropic in the plane of the substrate.

Most methods for determining the stress in a film are based upon measurement of the curvature of a uniformly coated substrate and the use of Eq. (19). Note that it is only necessary to know the thicknesses of the film and the substrate, and the elastic properties of the film; as long as it is of uniform and known thickness, it may have any composition and microstructure and the stress can still be obtained. Many methods have been used for the curvature measurement(X-ray[22] as well as various optical techniques), but a laser-based optical technique[23,24] provides the best combination of accuracy, convenience, and speed for the curvature measurement of anodic oxide films.

Figure 3 shows a laser-beam deflection ap-

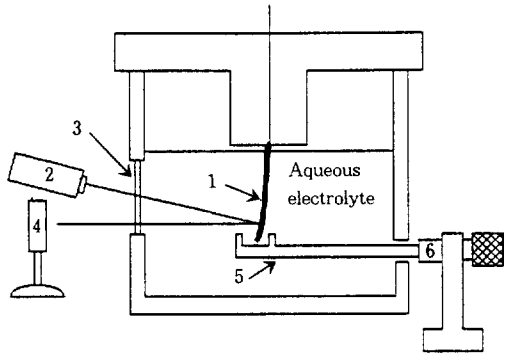

Fig. 3. A beam deflection apparatus used to measure stress development on the surface of metal : 1, specimen; 2, laser source; 3, flat window; 4, photocell; 5, stainless steel rod; 6, micrometer.

paratus used to measure the stresses generated during anodic oxidation of metals. It was based upon the method developed by Stoney,[23] later modified by Nelson and Oriani.[8,17] To follow the motion of the free end of the foil specimen 1 a laser beam from a laser source 2 is directed through a flat window 3 on the side of the cell, reflected off the mirror near the end of the strip, and back out through the window. The reflected beam is intercepted by a photocell 4 covered by a mask with a narrow horizontal slit cut in it. As the beam moves across the slit the changing light intensity allows monitoring of the motion at the end of the specimen. Calibration is achieved by pushing or pulling the free end of the specimen with a glass rod 5 attached to a micrometer 6. Some error is introduced here as the bending caused by the point load used in calibration is not equivalent to that due to the distributed load on the specimen surface. However, by offsetting the mirror slightly from the free end of the specimen, deflection measurements as small as 1μm can be made and errors can keep to less than 4%.

2.4 Effect of oxide growth rate on surface stresses in anodic oxide films

Vermilyea[4] firstly measured surface stresses in anodic oxide films on several metals by clamping the upper end of a thin foil of the metal specimen and observing the motion of the lower end through a telescope in an aqueous medium. In his work,[4] it was found that for most metals the sign of the stresses was independent of formation voltage and film thickness. From the experimental results, he considered that the sign of the stresses in anodic oxide film on a metal is a characteristic of the metal. However, the stress measurement was made on as-received specimen which would have

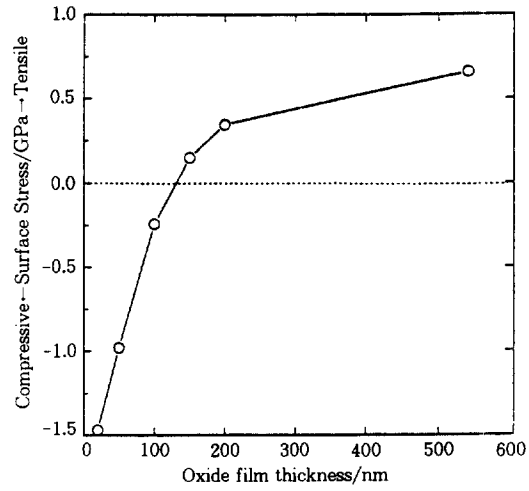

Fig. 4. Change in surface stress with oxide film thickness for an anodic oxidation of aluminium strip specimen at an applied current density of 3.3mA cm^{-2} in ammonium borate solution(pH=9.7) taken from Bradhurst and Leach.[5] Dotted line indicates the zero position of deflection.

residual stresses in itself. It is inferred that such stresses are relieved during the anodic oxidation and are overlapped with surface stresses generated by the anodic oxidation of metal. So it is questionable whether Vermilyea's work provides reliable data of the genuine surface stresses in the anodic oxide film.

Bradhurst and Leach[5] used a strip-deflection method to determine the stresses generated during the anodic oxidation of Al. Figure 4 shows the change in surface stresses with applied current density obtained from anodic oxidation of Al in pH 9 ammonium borate electrolyte. The stresses were dependent upon the applied current density : at lower current densities, the films were in compression, and at higher current densities tensile stresses were observed. The results(Fig.4) were explained by the work of Davis et al.[25] in which the transport number of cation in anodic oxide film on Al is changed from 0.33 to 0.72 with in-

creasing applied anodic current density from 0.1 to 10mA cm^{-2}. On the basis of the experimental results,[25] Bradhurst and Leach[5] ascribed the increasing movement in a tensile direction with increasing applied current density to the increasing number of cation vacancies remaining at the metal /oxide interface with increase of the rate of oxide growth.

Figure 5[18] shows the changes in surface stress with time calculated from the measured deflections produced during the anodic oxidation of tungsten at various current densities of 0.02 to 0.65 mA cm^{-2}. The stress-time curves exhibit two characteristics to be noticed. One is that the stresses move increasingly in a tensile direction, as the applied current density increased. The other is that more compressive stresses are built up at the earlier stage of anodic oxidation and become less compressive at the later stage.

Recognizing the fact that no significant variation in the cationic transport number of anodic tungsten oxide film with both applied current density and film thickness was observed,[25] it is not plausible to give reasons for the changes in the sign and rate of deflection with both applied current density and anodic oxidation time(Fig.5) in terms of the changes in the cationic transport number.

Kim et al.[18] demonstrated the experimental results(Fig.5) with respect to the electrochemical reactions occurring at the metal/oxide and the oxide/electrolyte interfaces. According to point defect model,[26] the electrochemical reactions occurring at the metal/oxide film interface are given by

$$M_M(m) = M_M(ox) + \nu/2\ V_O^{2+}(ox) + \nu e \quad (20)$$

and

$$M_M(m) + V_M^{\nu-}(ox) = M_M(ox) + \nu e \quad (21)$$

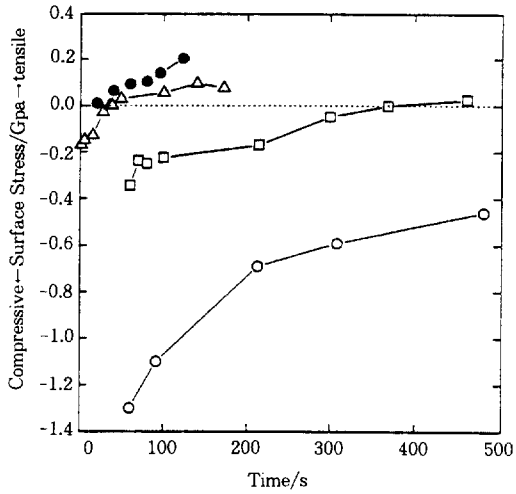

Fig. 5. Changes in surface stresses with time for anodic oxidation of tungsten strip specimen at applied current densities of : ○, 0.02mA cm^{-2} ; □, 0.05 mA cm^{-2}; △, 0.10 mA cm^{-2}; ●, 0.65mA cm^{-2}, taken from Kim et al.[18] Dotted line indicates the zero position of deflection.

where $M_M(m)$ represent the normal metal atom in the regular metal site, $M_M(ox)$ represent the normal metal ion in the regular site of the anodic oxide film, ν represent the charge number of the metal ion, $V_O^{2+}(ox)$ represent the positively charged oxygen vacancy, e represent the electron and $V_M^{\nu-}(ox)$ represent the negatively charged cation vacancy. The point defect model[26] also assumes the following two electrochemical equilibria at the oxide film/electrolyte interface:

$$V_O^{2+}(ox) + H_2O(aq) = 2H^+(aq) + O_O(ox) \quad (22)$$

and

$$M_M(ox) = V_M^{\nu-}(ox) + M^{\nu+}(aq) \quad (23)$$

where $H^+(aq)$ is the hydrogen ion in the aqueous electrolyte, $O_O(ox)$ is the normal oxygen ion in the regular site of the anodic oxide film and $M^{\nu+}(aq)$ is the charged metal ion in the aqueous electrolyte.

Considering that the conversion of a W atom into a W ion in the anodic oxide film on W substrate produces free volume equal to about 90% of the volume of the W atom at the metal/anodic oxide film interface, the effect of the production of free space due to the conversion of W atoms into W ions would be counterbalanced by the effect of the reduction in free space due to the annihilation of cation vacancies, as reaction (21) proceeds at the metal/oxide film interface. The contraction of the lattice spacing of the outermost layer of the anodic oxide film due to the formation of cation vacancies according to reaction (23) would be exceeded by its expansion due to the incorporation of the oxygen ions into the oxide film lattice according to reaction (22).

However, as reaction (20) proceeds, both the conversion of metal atoms into metal ions and the formation of oxygen vacancies in the anodic oxide film take place simultaneously at the metal/oxide interface. Thereby, a large amount of free space would be developed at the metal/oxide interface unless the generated oxygen vacancies are annihilated by the inward diffusion of oxygen ions formed at the oxide/electrolyte interface via reaction (22). This reasoning leads one to assert that reaction (20) is mainly responsible for the deflection behaviour encountered during the anodic oxidation of W.

It was reported[27] that activation energy for the diffusion of oxygen ions through the anodic oxide film on Fe substrate increases with increasing oxide film thickness. Thus, at very low film thickness, the oxygen vacancies formed by reaction (20) can be easily eliminated by the inward diffusion of the oxygen ions formed at the oxide/electrolyte interface according to reaction (22). Consequently, a compressive deflection probably occurs at the metal/oxide interface in the initial stage of the anodic oxidation of tungsten(Fig.5).

However, as the film grows, it is expected that it becomes more difficult for the oxygen vacancies to be eliminated due to the increase in the activation energy for the diffusion of oxygen ion through the anodic oxide film. A larger number of oxygen vacancies would build up at the metal/oxide interface with increase of the thickness of the anodic oxide film, leading to the transition from compressive to tensile deflection(Fig.5). Therefore, it was suggested[18] that the changes in the sign and magnitude of the stresses generated during the anodic oxidation of tungsten are crucially determined by how fast the oxygen vacancies formed at the metal/oxide interface are annihilated by the oxygen ions which move from oxide/solution interface toward the metal/oxide interface.

The explanation of the effect of current density on the stress generation in terms of relevant electrochemical reactions responsible for anodic oxide film growth is applicable to not only W but also various metals such as Al,[3, 5] Zr[7, 28] and Ti,[29] and is also helpful for us to understand the mechanism of stress relief during anodic oxidation of metals.

2.5 Effect of anion impurity on surface stresses in anodic oxide films

It was reported,[7, 8, 30, 31] that anion impurities of electrolyte such as halide ion greatly affect surface stresses generated during the anodic oxidation of metals. However, there is still controversy concerning the influence of halide ion on the generation of the stresses in anodic oxide film of metals. Archibald and Leach[7,30] showed that if Zr is electropolished in the HF-free solution, the stresses developed during the anodic oxidation are

always compressive whereas if Zr is etched in the HF-containing solution the surface stresses in the initial stage of the anodic oxidation are tensile and then become compressive. They attributed the initial tensile stresses to the increased cation migration due to the F^-left on the metal substrate during the chemical polishing. However, they left the reason why the compressive stresses develop in the later stage of the anodic oxidation.

In contrast, Nelson and Oriani reported[8] that much larger compressive stresses are developed in the anodic oxide film on nickel grown in Cl^--containing solution than in Cl^--free solution. They attributed the larger compressive stresses to the larger volume of Cl^-than that of O^{2-}incorporated in the oxide film.

Quarto et al.[31] found that the values of the breakdown voltage and dielectric constant of anodic oxide film on W are greatly influenced by the incorporation of anion impurities in the anodic oxide film, and regarded that changes in defect structure of anodic oxide films with anion impurities are very significant in determining the values of surface stresses developed during anodic oxidation of metals.

Kim et al.[32] investigated the surface stresses developed during the anodic oxidation of W as a function of Cl^- and applied current density, based upon the idea that both the changes in defective structure and in growth kinetic behaviour actually contribute to the magnitude and the sign of the surface stresses of metal. Figure 6[32] shows that the changes in surface stresses with time calculated from the measured deflections produced during the anodic oxidation of W at an applied current density of 0.08 mA cm^{-2} in 0.1 M H_2SO_4 solutions containing various [Cl^-] of 0 to 0.5 M by using Eq.(19).

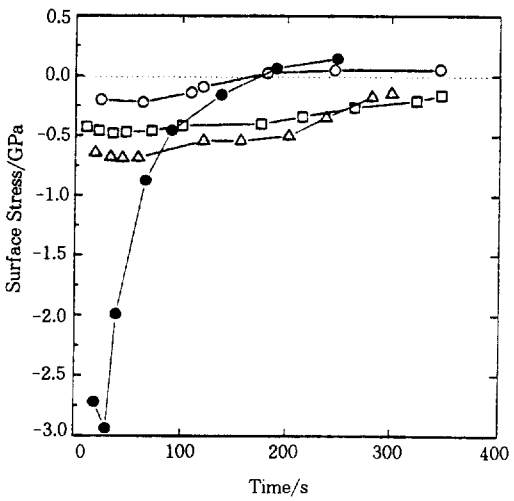

Fig. 6. Changes in surface stress with time during anodic oxidation of tungsten at an applied current density of 0.08 mA cm^{-2} in 0.1M H_2SO_4 solutions containing various concentrations of : ○, 0 M NaCl; □, 0.05 M NaCl; △, 0.10 M NaCl; ●, 0.50 M NaCl.

The experimental results(Fig.6) are also discussed with respect to growth related electrochemical reactions occurring both at the metal/oxide film interface and at the oxide film/electrolyte interface, and it is suggested that the stress increases in a compressive direction with chloride ion before the oxide film breakdown are attributed to the increase in PBR due to the incorporation of chloride ion in the oxide film. In contrast, after the oxide film breakdown the stress increases in tensile direction are due to the saturation of cation vacancies at the metal/oxide film interface.

3. Conclusion

From this review, it can be concluded that generation of surface stresses in anodic oxide films involves the transport of both oxygen ions and metal ions or their respective vacancies from the metal/

oxide film interface through the oxide film or from the oxide film/solution interface into the bulk oxide film. Thus, surface stresses developed during anodic oxidation of metals are important in determining the various properties of anodic oxide films on metals: structures of the oxide film, the mechanism of film formation and breakdown, and electrical and mechanical properties. In this respect, the achievement of an improved understanding of the stress generation mechanism is necessary for engineering applications of anodic oxide films on metals. Various important parameters affecting surface stress generation that can be investigated by stress measurements are summarized as follows:

1) The effects of applied anodic current density/anodic potential (current/potential step within passivation range, cyclic voltammetry)
2) The effect of time of passivation
3) The effect of electrolyte composition(changes in pH and halide ion concentration)
4) The effect of H^+ or Li^+ charging into anodic oxide films on transition metals.
5) The changes in stresses in electrodeposited layer during electrodeposition process.

Many of concepts developed for the stress generation in anodic films will also be applicable to thin films produced by deposition processes and oxides grown at high temperatures.

References

1. Hans L. Hartnagel, "Oxidation of semiconductor surfaces", in Oxides and Oxide Films, Vol. 6, 1st ed. P.85, A. K. Vijh(ed.), Marcel Dekker, New York, U. S. A., 1981.
2. P. Delichere, P. Falaras, M. Froment and A. H. Goff, Thin Solid Films, **161**, 35 (1988).
3. J. S. L. Leach and B. R. Pearson, Corrosion Science, **28**, 43 (1988).
4. D. A. Vermilyea, J. Electrochem. Soc., **110**, 345 (1963).
5. D. H. Bradhurst and J. S. L. Leach, J. Electrochem. Soc., **113**, 1245 (1966).
6. J. Stringer, Corros. Sci., **10**, 513 (1970).
7. L. C. Archibald and J. S. L. Leach, Electrochim. Acta., **22**, 15 (1977).
8. J. C. Nelson and R. A. Oriani, Electrochim. Acta, **37**, 2051 (1992).
9. N. B. Pillings and R. E. Bedworth, J. Inst. Metals, **29**, 529 (1923), cited in ref.5.
10. O. Kubaschewski and B. E. Hopkins, Oxidation of Metals and Alloys, 2nd ed., Butterworths, London, U. K., 1965, cited in ref.6.
11. A. T. Fromhold, Jr., Surf. Sci., **22**, 396 (1972).
12. R. P. Feynman, R. B. Leighton and M. Sands, Lectures on Physics(II), 1st ed., Addison-Wesley Publishing Company, Massachusetts, U. S. A., 1989.
13. G. E. Dieter, Mechanical Metallurgy, 3rd ed., P.18, McGraw-Hill Book Company, New York, U. S. A., 1986.
14. A. T. Fromhold, Jr., J. Chem. Phys., **51**, 1143 (1969).
15. W. D. Kingery, H. K. Bowen and D. R. Rhlmann, Introduction to Ceramics, 2nd ed., P. 931, John Wiley & Sons, New York, U. S. A., 1976.
16. R. W. Hertzberg, Deformation and Fracture Mechanics of Engineering Materials, 2nd ed., P.8, John Wiley & Sons, New York, U. S. A., 1983.
17. J. C. Nelson and R. A. Oriani, Corros. Sci., **34**, 307(1993).
18. J.-D. Kim, S. -I. Pyun and R. A. Oriani, press in Electrochim. Acta,1995.
19. J. L. Ord, J. C. Clayton and K. Byudzewski, J.

Electrochem. Soc., **129**, 908(1978).

20. P. A. Flinn, D. S. Gardner and W. D. Nix, IEEE Trans., **ED-34**, 689(1987).
21. U. A. Brantley, J. Appl. Phys., **44**, 534(1973).
22. A. Segmuller, J. Angilelo and S. J. LaPlaca, J. Appl. Phys., **51**, 6224(1980).
23. G. G. Stoney, Proc. Roy. Soc. **A82**, 172(1909), cited in ref.6.
24. A. K. Sinha, H. J. Levenstein and T. E. Smith, J. Appl. Phys., **49**, 2423(1984).
25. J. A. Davis, B. Domeij, J. P. S. Pringle and F. Brown, J. Electrochem. Soc., **112**, (675)1965.
26. C. Y. Chao, L. F. Lin and D. D. Macdonald, J. Electrochem. Soc. **128**, 1187(1981).
27. N. Sato and M. Cohen, J. Electrochem. Soc., **111**, 512(1964).
28. V. R. Howes, Corros. Sci. **14**, 491(1974).
29. L. C. Archibald, Electrochim. Acta, **22**, 657 (1977).
30. L. C. Archibald and J. S. L. Leach, Electrochim. Acta., **22**, 21(1977).
31. F. Di Quarto, A. Di Paola and C. Sunseri, J. Electrochem. Soc., **27** 1016 (1980).
32. J.-D. Kim, S. -I. Pyun and R. A. Oriani, accepted for publication in Electrochim. Acta, 1995.